Chapter 4

Results and discussion

In this chapter, the concentrations of criteria pollutants (Par. 4.2. – Par.4.6.) i.e. SO_2, NO_2, O_3, CO and PM_{10} measured in the BIC are compared to South African and European standards. The diurnal and seasonal concentration patterns of these species are presented and discussed. Possible sources of these species in the region where monitoring was conducted are also identified. Finally, general conclusions (Par. 4.7.) are made with regard to general air quality in the western Bushveld Igneous Complex from results obtained in this investigation.

4.1. Introduction

The experimental data obtained during the sampling period for SO_2, NO_2, O_3, CO and PM_{10} are compared to current South African and European standards. The exceedances that are reported were calculated for the entire dataset, i.e. for two years, three months and nine days, which were then converted to obtain annual exceedances. In subsequent paragraphs, each individual pollutant is discussed in terms of legislative implications, observed patterns (e.g. diurnal and seasonal) and possible sources.

In Table 4.1, the National Ambient Air Quality Standards are compared with European ambient air quality standards. As can be seen, the standards are very similar, differing only in the amount of tolerated exceedances per year.

Table 4.1: Ambient air quality standards based on the South African National Environment Management: Air Quality Act (NEM:AQA, 2004)

		South African standards		European standards	
Pollutant	**Averaging period**	**Concentration [ppb] (µg/m^3)**	**Tolerable Exceedance per year**	**Concentration [ppb] (µg/m^3)**	**Tolerable exceedance per year**
SO_2	10 min	191 (500)	526		
	1 hour	134 (350)	88	134 (350)	24
	24 hour	48 (125)	4	48 (125)	3
	1 year	19 (50)	0		
NO_2	1 hour	106 (200)	88	106 (200)	18
	1 year	21 (40)	0	21 (40)	n/a
O_3	8 hours (moving from 1 hour ave)	61 (120)	11	61 (120)	n/a
CO	1 hour	26000 (30000)	88		
	8 hour (moving from 1 hour ave)	8700 (10000)	11	8700 (10000)	n/a
PM_{10}	24 hours	120	4	50	35
	24 hours (2015)	75	4		
	1 year	50	0	40	n/a
	1 year (2015)	40	0		

4.2. SO_2

In Table 4.2, the SO_2 concentrations measured during the entire sampling period are compared to ambient standards. SO_2 had a mean 10 minute average concentration of 3.8ppb (9.9µg/m³) during the sampling period. A maximum 10 minute average of 245.9ppb (639.9µg/m³) was measured that exceed the 191ppb (500 µg/m³) South African standard on average 3.96 times per year. The measured 1-hour average concentration for SO_2 had a maximum level of 140.3ppb (366.4 µg/m³), which exceeded the South African

and European standard of 134ppb (350 µg/m³). This maximum was a once-off exceedance of the standards for the entire sampling period (0.44 p.a.), which was well below the 88 and 24 tolerable exceedances allowed annually by the South African and European legislation, respectively. The maximum 24-hour average concentration of 20.8ppb (54.3µg/m³) was below the 48ppb (125µg/m³) air quality South African and European standard. The average annual concentration for the entire sampling period was 3.8ppb (9.9 µg/m³), which is well below the 19ppb (50µg/m³) limit allowed by South African law.

Table 4.2: Comparison of measured SO_2 data to South African and European air quality standards listed in Table 4.1

	Measurements					
Averaging period	**Average exceedances per year**		**Sampling period max [ppb] (µg/m³)**	**Sampling period min [ppb] (µg/m³)**	**Sampling period average [ppb] (µg/m³)**	**% data coverage**
	SA	**EUR**				
10 min	3.96		245.9 (639.9)	0	3.8 (9.9)	85
1 hour	0.44	0.44	140.3 (366.4)	0		
24 hour	0	0	20.8 (54.3)	0.1 (0.3)		
1 year	0		4.1 (10.8)	3.6 (9.4)		

In Figure 4.1, the diurnal seasonal concentration pattern is shown. It is clear that SO_2 concentrations peaked between 07:30 and 10:00 irrespective of the season, with concentrations during winter being the highest. The late morning SO_2 peak indicates that SO_2 is not associated with the cooking and space-heating practices of the semi- and informal settlements in the area. If this were the case, two SO_2 peaks would have been expected; one in the early morning (e.g. 06:00 to 07:00) and one in the early evening (e.g.

18:00 to 20:00). The observed late morning SO_2 peak rather correlates with the break-up of the low-level inversion layer that forms quite regularly in the South African Highveld. The formations of several well-developed inversion layers, at different heights, typically form during the night and persist until late morning (Garstang *et al.*, 1996; Tyson *et al.*, 1996; Wenig *et al.*, 2003). These low-level inversion layers are especially strong in winter. Therefore, the timing of the diurnal seasonal SO_2 patterns indicates high-stack emission sources of SO_2. It is known that the PGM industry in this area has relatively high SO_2 emissions, since this industry utilises sulphite ore (Xiao & Laplante, 2004) that generate substantial SO_2 emissions. High stack SO_2 emissions can accumulate between two inversion layers during night time, which is then released after the break-up of the inversion layers in the morning, hence resulting in an SO_2 peak at ground level. The higher SO_2 concentration peak observed during winter can be ascribed to the fact that the formation and persistence of the inversions layers are more pronounced in winter (Garstang *et al.*, 1996; Tyson *et al.*, 1996; Wenig *et al.*, 2003). Further proof that the single diurnal SO_2 peak can be related to the trapping and release of pollution from high stacks is indicated by the timing of the peaks during the different seasons. The persistence of the inversion layers in winter is indicated by the fact that the winter SO_2 peak occurs somewhat later than in the other seasons. Higher SO_2 concentrations in the winter can most probably be ascribed to additional SO_2 from biomass burning on a regional scale in southern Africa, as well as regional recirculation of pollutants, especially during the dry winter months (Tyson *et al.*, 1996). These additional, non-local sources only manifest after the break-up of the low-level inversion layers in late morning.

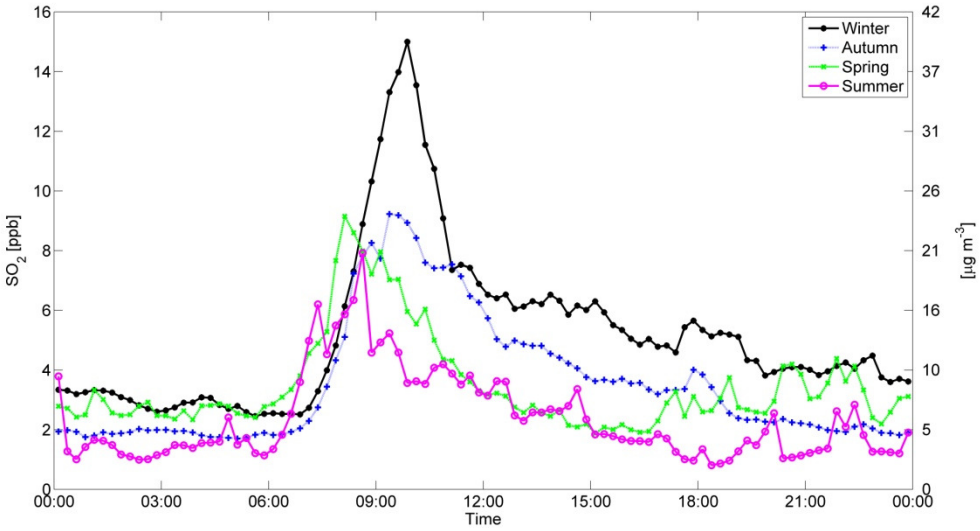

Figure 4.1: Mean diurnal seasonal concentration distribution of SO_2 (Winter: June, July, August; Spring: September, October, November; Summer: December, January, February; Autumn: March, April, May)

In an effort to correlate the SO_2 measurements with specific sources or source sectors in the western BIC, a pollution rose for SO_2 measured during 12:00 and 16:00 (red) was compiled in addition to a pollution rose for the entire sampling period (black). During this time of day (12:00-16:00) the atmosphere is expected to be relatively well mixed, making it possible to correlate measured pollutant concentrations with wind direction. In Figure 4.2, pollution roses for SO_2 and NO_2 measured are shown. The SO_2 12:00-16:00 pollution rose (red) shows a dominance of sources from the west-north-west to the north-north-west, as well as the east-north-east to the south-east sectors. As can be seen in Figure 3.1, the southern section of the western BIC (south of the Pilanesberg crater) and the associated placement of pyrometallurgical smelters, has a greater spatial expanse from east to west, than north to south. The shape of the SO_2 pollution rose mimics this east-west dominance, again confirming the SO_2 contribution from the high stack emissions.

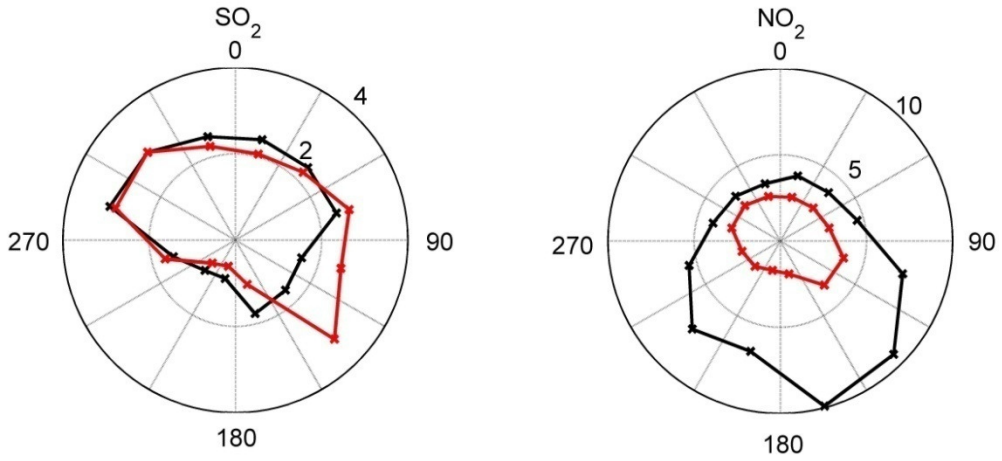

Figure 4.2: Pollution roses for SO_2 and NO_2

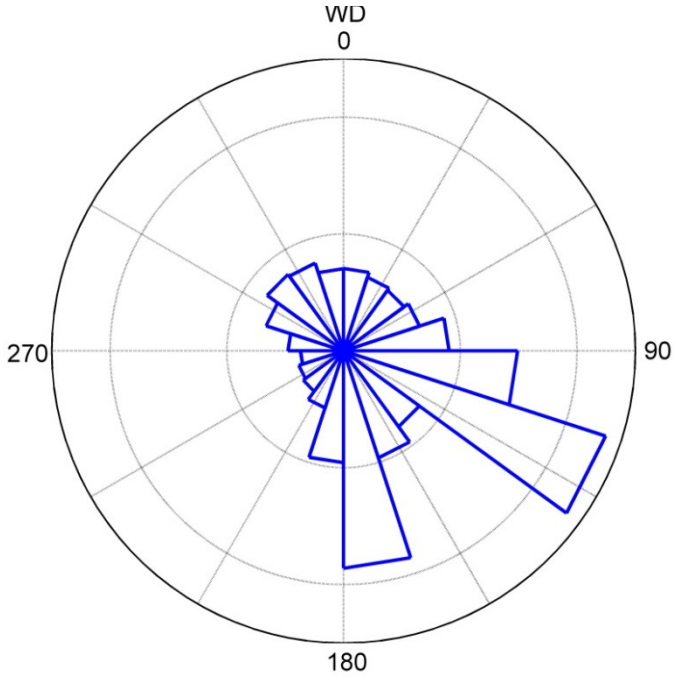

Figure 4.3: Mean wind rose indicating the dominant wind direction

Figure 4.3 indicates the mean wind rose for the entire sampling period. As can be seen, the dominant wind directions are between south and east. This also shows one of the source regions with higher SO_2 concentrations (Figure 4.2), hence the site is frequently impacted by SO_2 from that source area.

In Figure 4.4, the diurnal trend for SO_2 is presented for each day of the week. These patterns were calculated for the entire sampling period. The same SO_2 trend is observed every day of the week. This again confirms that SO_2 mainly originates from metallurgical industrial sources, since these smelters are operated continuously (see high stack emissions and inversion layer break-up as discussed on page 49).

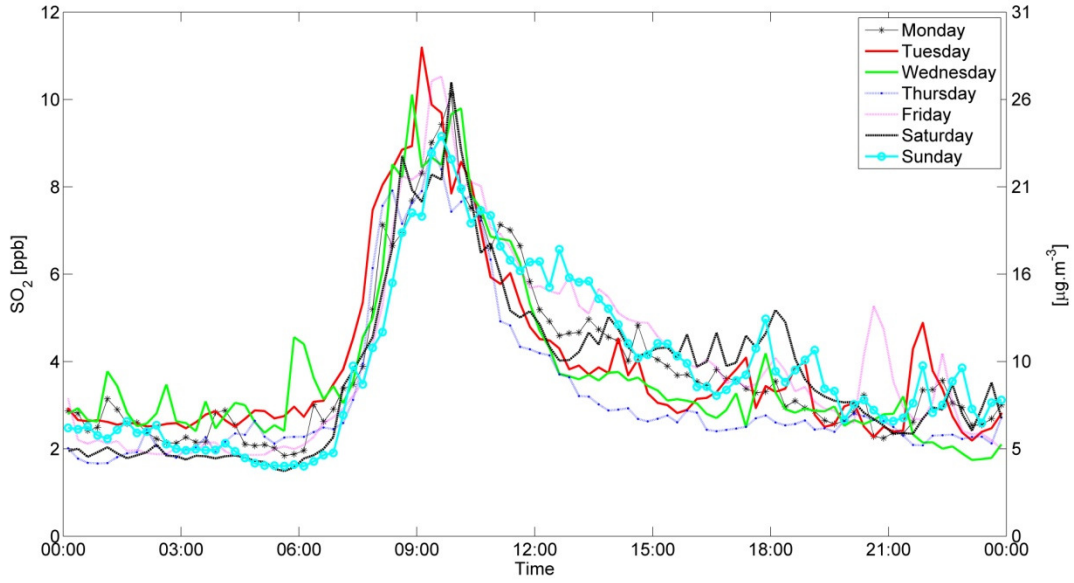

Figure 4.4: Mean daily diurnal SO_2 concentrations

4.3. NO_2

In Table 4.3, NO_2 levels are compared to legislative standards. A one-hour standard and an annual standard are prescribed for NO_2 ambient concentrations according to South African and European legislation. No exceedances of NO_2 standards were observed (Table 4.3). The mean 1-hour average was 8.5ppb (15.9 µg/m³), with a maximum of 68.88ppb (120.9µg/m³) that is below the 106ppb (200µg/m³) standard. The maximum annual concentration was 9.4ppb (17.7 µg/m³), which was also below the 21ppb (40µg/m³) legislative level. Data coverage for NO/NO_x is less than that of the other pollutants measured, this is due to data considered not entirely trustworthy being excluded.

Table 4.3: Comparison of measured NO_2 data to South African and European air quality standards listed in Table 4.1

	Measurements					
Averaging period	**Average exceedances per year**		**Sampling period max [ppb] (µg/m³)**	**Sampling period min [ppb] (µg/m³)**	**Sampling period average [ppb] (µg/m³)**	**% data coverage**
	SA	**EUR**				
1 hour	0	0	63.9 (120.9)	0	8.5 (15.9)	59
1 year	0	0	9.4 (17.7)	7.9 (17.9)		

In Figure 4.5, the diurnal seasonal trends for NO_2 are shown. NO_2 concentrations showed two distinctive peaks irrespective of the season. The first peak occurred between 06:00 and 10:00, while a second peak was observed between 17:00 and 22:00.

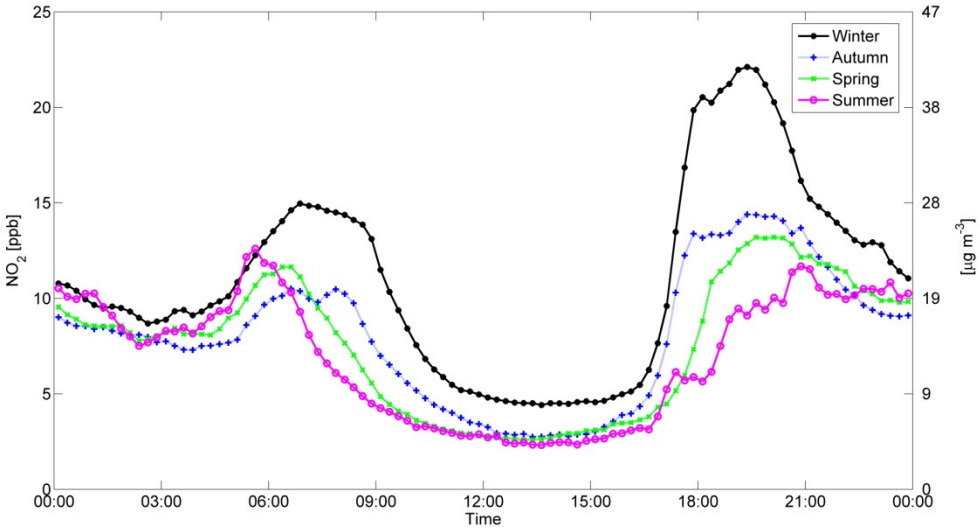

Figure 4.5: Mean diurnal seasonal NO_2 trends (Winter: June, July, August; Spring: September, October, November; Summer: December, January, February; Autumn: March, April, May)

Possible sources of NO_2 in this region include vehicular emissions, household combustion and pyrometallurgical smelters. The two diurnal NO_2 peaks observed (Figure 4.5) are characteristic of urban areas dominated by traffic emissions of NO_2, with NO_2 levels peaking in the early mornings and late afternoons during peak traffic hours. Traffic volumes are far less over weekends; hence this must be reflected by the onsite NO_2 measurements, if traffic was the main contributor to NO_2. However, investigation of separate average daily NO_2 diurnal cycles for each day of the week for the entire sampling period indicated that only Sundays had somewhat lower NO_2 concentrations (Figure 4.6). It is expected that traffic emissions would be lower on both Saturdays and Sundays. Therefore, these diurnal peaks would most likely also be less pronounced on Saturdays if traffic emissions were the main source of NO_2 at the measurement site. Additionally, the N4 highway is directly to the south of the site, which does not correlate to the dominant source regions indicated by the pollution rose measured from 12:00 to 16:00 for the entire sampling period (Figure 4.2). Therefore, it seems unlikely that vehicular emissions are the predominant source of NO_2 at this site.

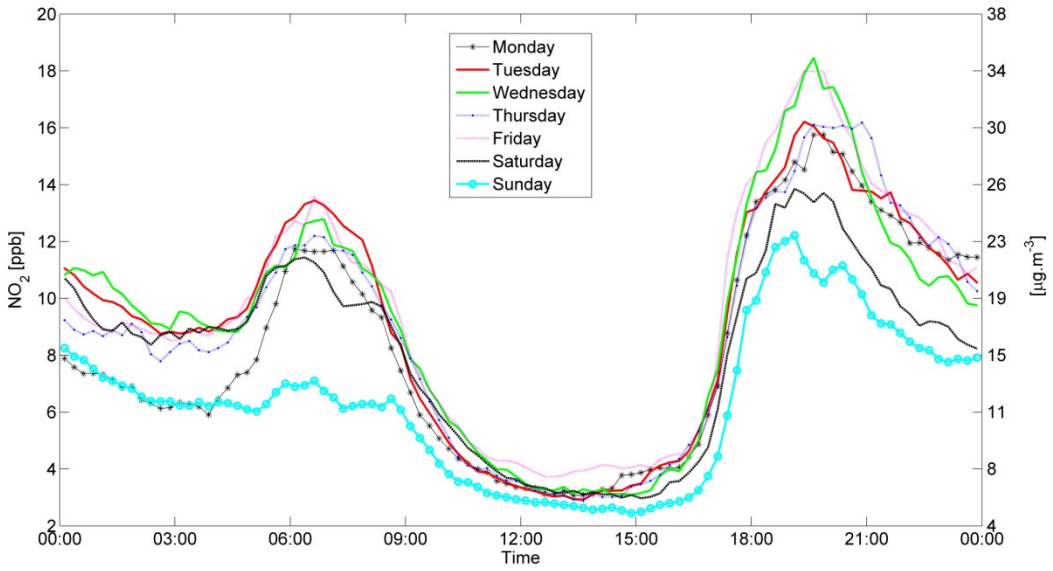

Figure 4.6: Mean daily diurnal NO_2 concentrations

The diurnal seasonal NO_2 peaks (Figure 4.5) can most likely be associated with household combustion, i.e. cooking and space heating, which have the same peak periods (morning and later afternoon into the evening) as traffic emissions. The more pronounced second diurnal NO_2 peak in winter indicates that household combustion is most likely the principal source of NO_2 at this site. During winter, there is an increase in biomass burning for space heating purposes, especially during night time. The seasonal variation observed in the diurnal trend, i.e. increase from summer to winter, can be attributed to the increased use of space heating during colder periods, compounded by the formation of low-level inversion layers during the colder months trapping low-level emissions. The NO_2 pollution rose measured from 12:00 to 16:00 for the entire sampling period (Figure 4.2) indicates a dominance of sources from the western and eastern to the south-eastern sectors. This correlates with the location of human settlements, immediately surrounding the measurement site (Figure 3.1), reinforcing the deduction that household combustions for cooking and space heating are the dominant sources. The lower diurnal NO_2 cycle observed for Sundays (Figure 4.6) can most likely be attributed to the fact that

most people tend to sleep later on Sunday, hence also reduced and delayed early morning space heating and cooking activities.

Other combustion processes in this area, e.g. pyrometallurgical smelters, can also contribute to observed NO_2 levels. However, it is evident that high-stack emissions from industries are not the main source of NO_2. If this was the case, NO_2 would have peaked after the morning break-up of the low-level inversion layers, as was observed for SO_2. Such a situation was observed by Collett *et al.* (2010), who reported that NO_2 peaked after the break-up of the low-level inversion layers in the morning, as a result of the dominance of NO_2 high-stack emissions from coal-fired power stations in the Highveld Priority Area (Collett *et al.*, 2010).

4.4. O_3

According to South African and European standards, O_3 only has an eight-hour moving average concentration standard of 61ppb (120µg/m³). The eight-hour moving average (calculated from moving one-hour averages) is compared to South African and European standards in Table 4.4. South African legislation allows 11 tolerable exceedances per year, while European standards have no indication of tolerable exceedances. The highest eight-hour moving average O_3 concentration measured was 112ppb (224µg/m³), while the mean eight-hour moving average O_3 concentration was 29.2ppb (58.2µg/m³). As can be seen from Figure 4.7, the 61ppb limit concentration was exceeded on 732 instances (average of 322 p.a.) during the sampling period, which clearly signifies the magnitude of O_3 pollution in this area.

Table 4.4: Comparison of measured O_3 data to South African and European air quality standards listed in Table 4.1

Averaging period	Measurements					
	Average exceedances per year		Sampling period max [ppb] ($\mu g/m^3$)	Sampling period min [ppb] ($\mu g/m^3$)	Sampling period average [ppb] ($\mu g/m^3$)	% data coverage
	SA	EUR				
8 hours (moving from 1 hour ave)	322.24	n/a	112 (224)	0.9 (1.8)	29.1 (58.2)	87

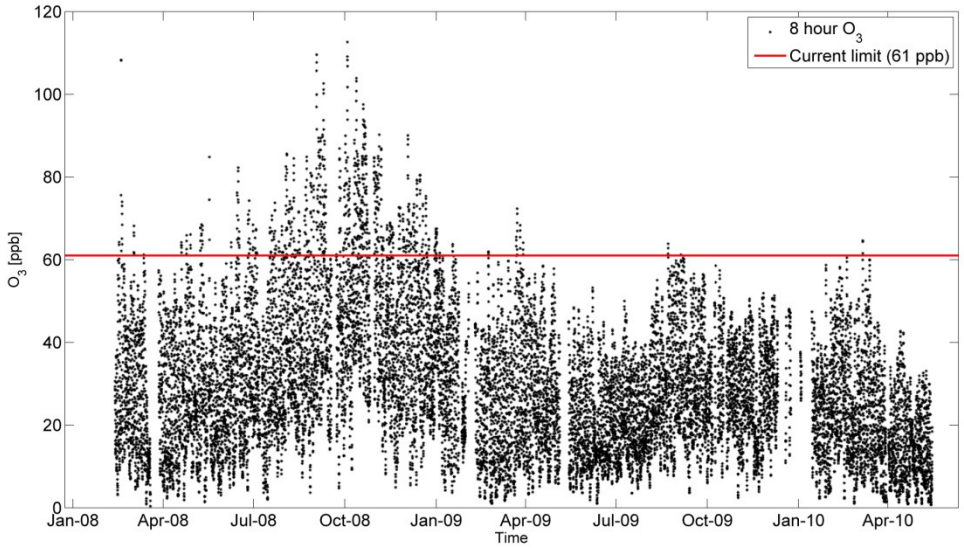

Figure 4.7: The 8 hour moving averages of O_3 exceeding the 61 ppb limit

In Figure 4.9, the mean diurnal seasonal trends for O_3 are presented. As expected, O_3 depicts a peak during daytime, since O_3 formation is dependent on solar radiation. In Figure 4.14, the diurnal seasonal global radiation measured during the sampling period is

shown. Solar radiation peaked at approximately 13:00, which preceded the O_3 peak that occurred between 14:00 and 16:00.

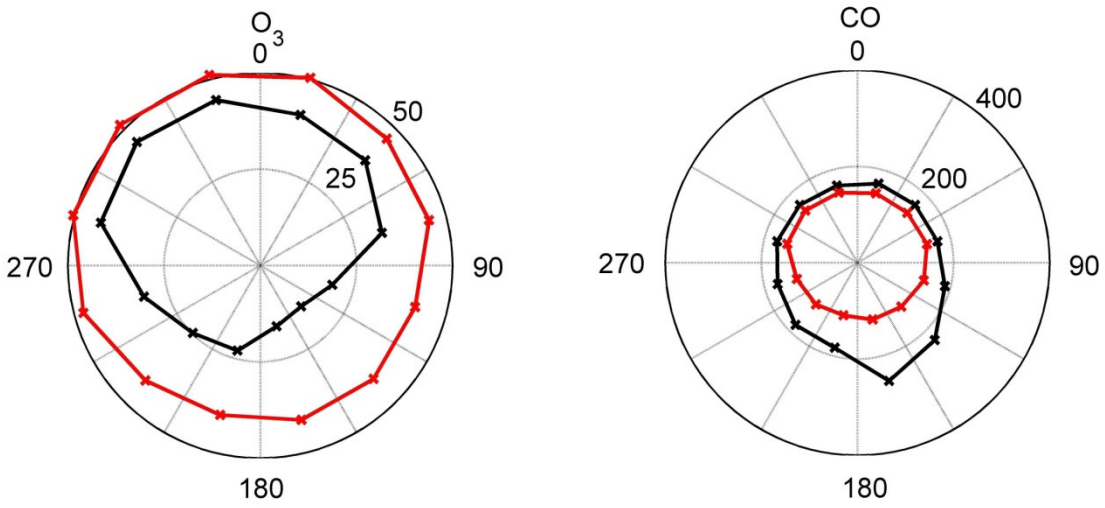

Figure 4.8: Pollution roses for O_3 and CO

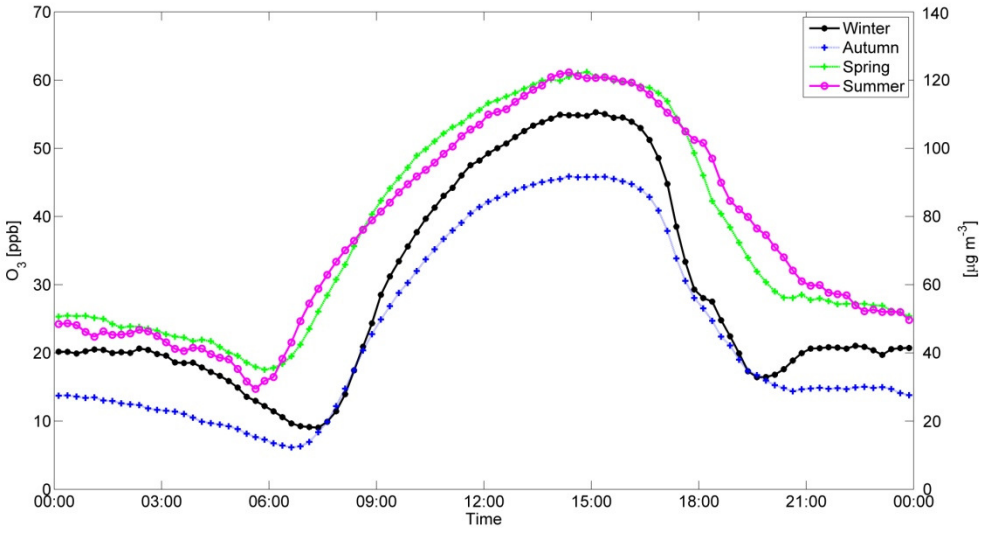

Figure 4.9: Mean diurnal seasonal trends for O_3 (Winter: June, July, August; Spring: September, October, November; Summer: December, January, February; Autumn: March, April, May)

The diurnal seasonal patterns of O_3 indicate the highest O_3 concentrations during spring. This seasonal trend was also observed in recent measurements in the interior of South Africa (Josipovic *et al.*, 2010; Laakso *et al.*, 2010; Lourens *et al.*, 2011(a)). O_3 is a secondary pollutant and the conversion of O_3 precursors occurs during air transport from source regions. Figure 4.10 shows the hourly 96-hour overlay back trajectories for Marikana with a 100m arrival height for the entire sampling period. The black lines in Figure 4.10 are contour time lines that indicate the average trajectory position in each direction at a given time. From this figure, it is clear that the Highveld Priority Area, with its high NO_2 levels (Collett *et al.*, 2010), is on the dominant anti-cyclonic regional recirculation path of Marikana. This at least partially explains the regular exceedances of O_3 standards. Additionally, the higher O_3 levels observed during spring can also be explained by regional, rather than local, sources (Figure 4.9). Laakso *et al*. (2008) found CO, also a known precursor for O_3, to peak during early spring at Botsalano, 175km west-north-west from Marikana, which is also on the anti-cyclonic regional recirculation path of Marikana. Higher CO concentrations during spring are most likely associated with regional biomass burning events in southern Africa (Swap *et al.*, 2003).

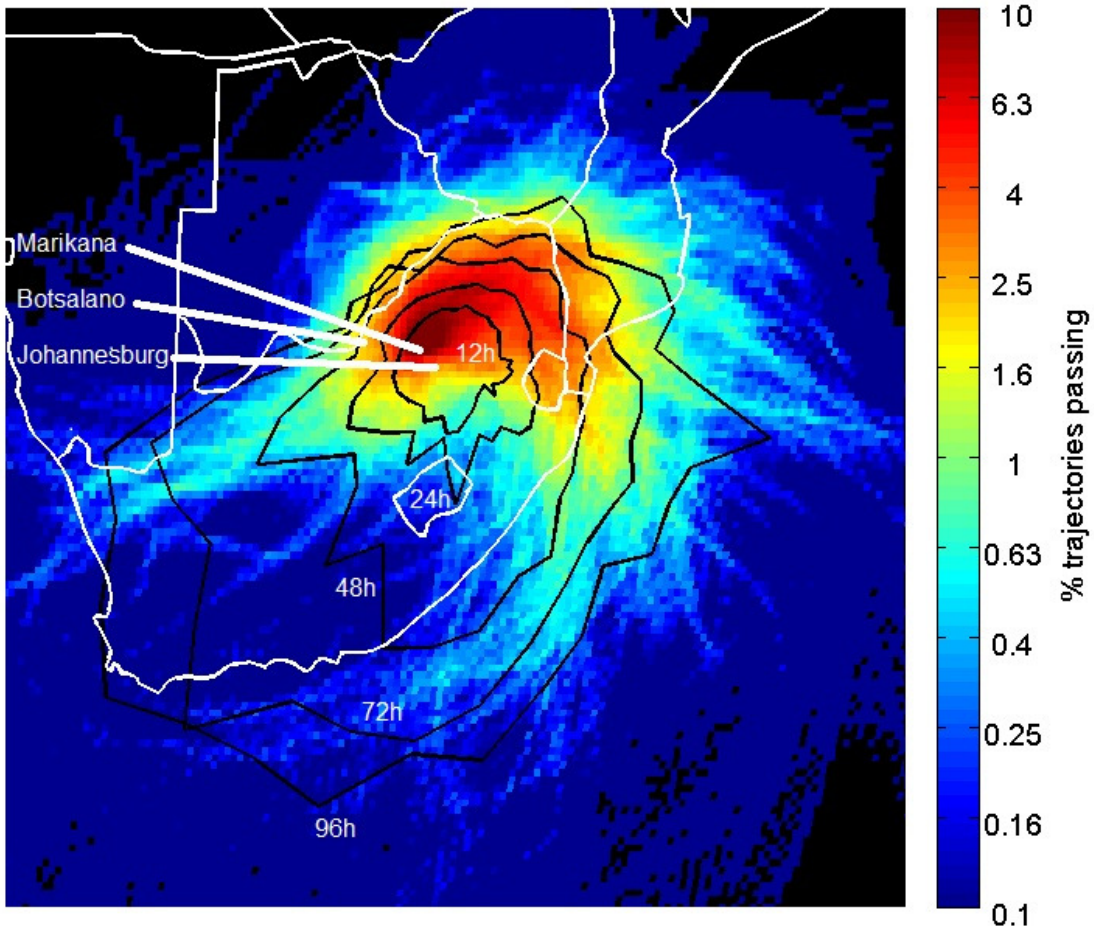

Figure 4.10: Hourly 96-hour overlay back trajectories with 100m arrival height for the entire sampling period arriving at Marikana

Attributing the O_3 levels at Marikana mostly to regional, rather than local, sources, is also supported by other meteorological parameters, i.e. wind speed, temperature and relative humidity, shown in Figure 4.11-4.14. Wind speed is highest in spring, which can result in accelerated transport of aged regional air parcels. The temperature and relative humidity of diurnal seasonal trends indicate that the atmosphere during spring is almost as hot as summer and dry as winter, which is conducive to biomass burning.

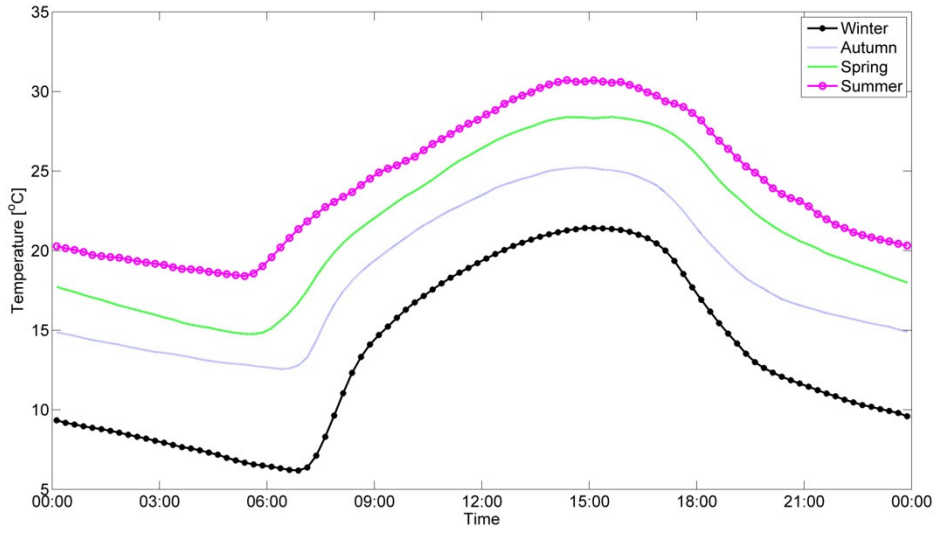

Figure 4.11: Mean diurnal seasonal trends depicting the temperature differences

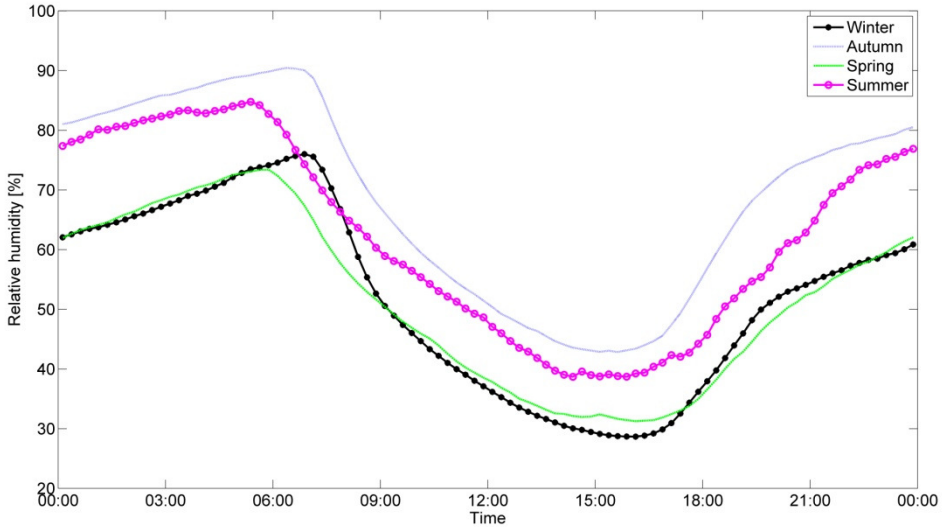

Figure 4.12: Mean diurnal seasonal trends of the relative humidity

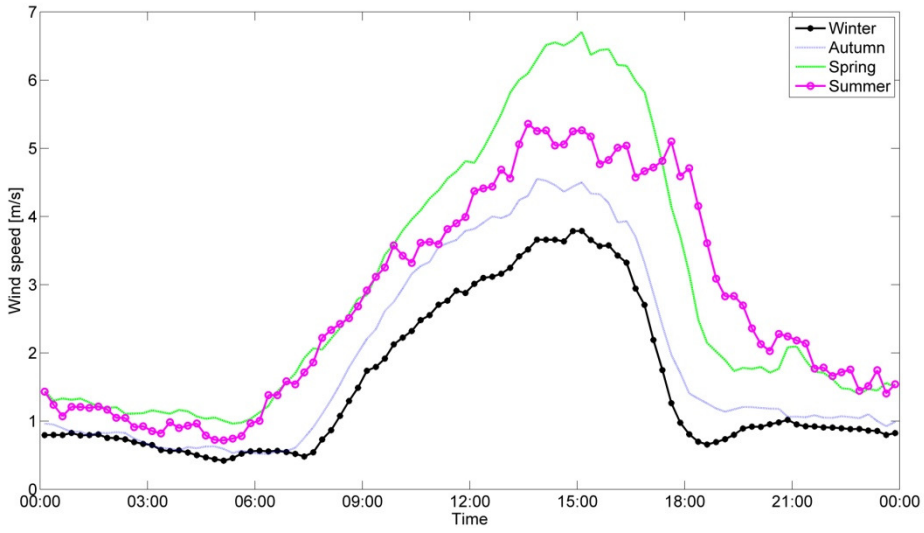

Figure 4.13: Mean diurnal seasonal trends showing the increase in wind speeds during spring and summer months, leading to an increase in vertical mixing

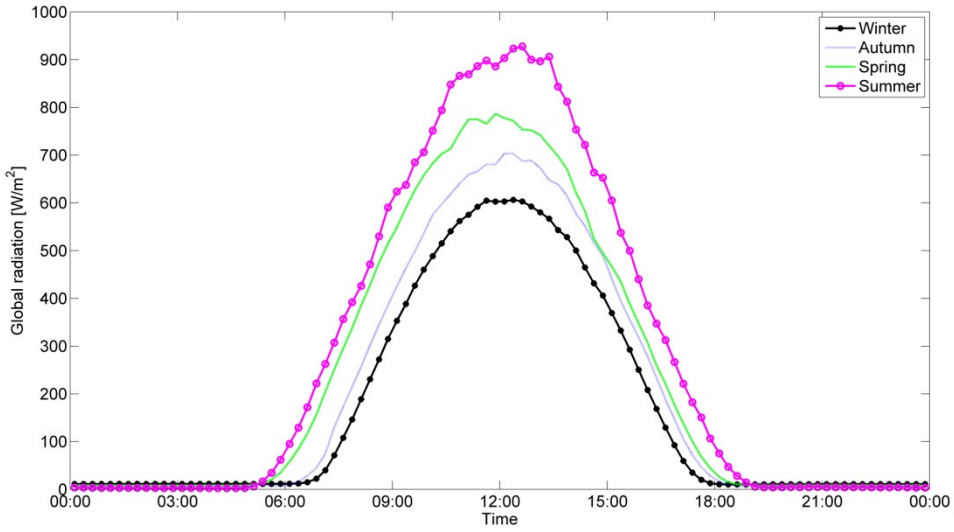

Figure 4.14: Mean diurnal seasonal global radiation measured during the sampling period

4.5. CO

The maximum measured one-hour average concentration for CO was 1910ppb (2200µg/m³), which did not exceed the South African standard of 2600ppb (3000µg/m³). CO concentrations obtained during this investigation are compared to standard levels in Table 4.5. The mean one-hour average concentration was 230ppb (270µg/m³) for the entire sampling period. The eight-hour moving average (calculated from one-hour averages) had a maximum of 880ppb (1020µg/m³), which did not exceed the 8700ppb (10000µg/m³) South African and European standard.

Table 4.5: Comparison of measured CO data to South African and European air quality standards listed in Table 4.1

	Measurements					
Averaging period	**Average exceedances per year**		**Sampling period max [ppb] (µg/m³)**	**Sampling period min [ppb] (µg/m³)**	**Sampling period average [ppb] (µg/m³)**	**% data coverage**
	SA	**EUR**				
1 hour	0		1910 (2200)	40 (50)	230 (270)	86
8 hour (moving from 1 hour ave)	0	n/a	880 (1020)	60 (70)		

In Figure 4.15, the diurnal seasonal patterns for CO are shown. Similar to NO_2, CO also shows a peak between 06:00 and 10:00, as well as a second peak between 17:00 and 22:00. If high-stack emissions from pyrometallurgical smelters were the dominant contributor to CO levels, a single peak in the morning after the break-up of the low-level inversion layers would have been observed (similar to SO_2). The diurnal CO peaks correspond with typical periods for household combustion, which is also verified by the more pronounced second diurnal CO peak (17:00-22:00) in winter when space heating is mostly applied.

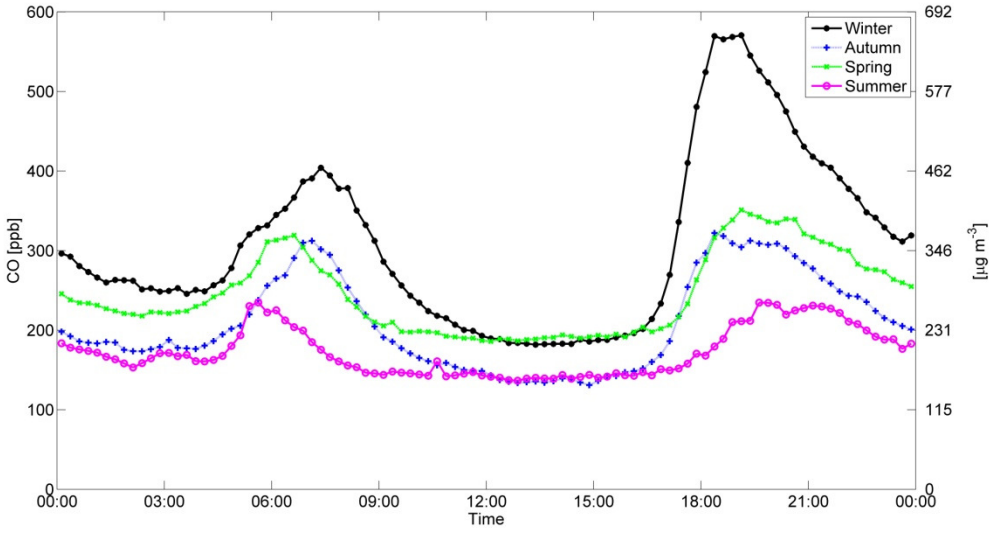

Figure 4.15: Mean diurnal seasonal patterns for CO (Winter: June, July, August; Spring: September, October, November; Summer: December, January, February; Autumn: March, April, May)

In Figure 4.16, the diurnal patterns for CO concentrations are shown for each day of the week. It is evident from Figure 4.6 that a similar trend is observed as the pattern obtained for NO_2 concentrations. This also further confirms the conclusion that CO emissions were mainly from household combustion.

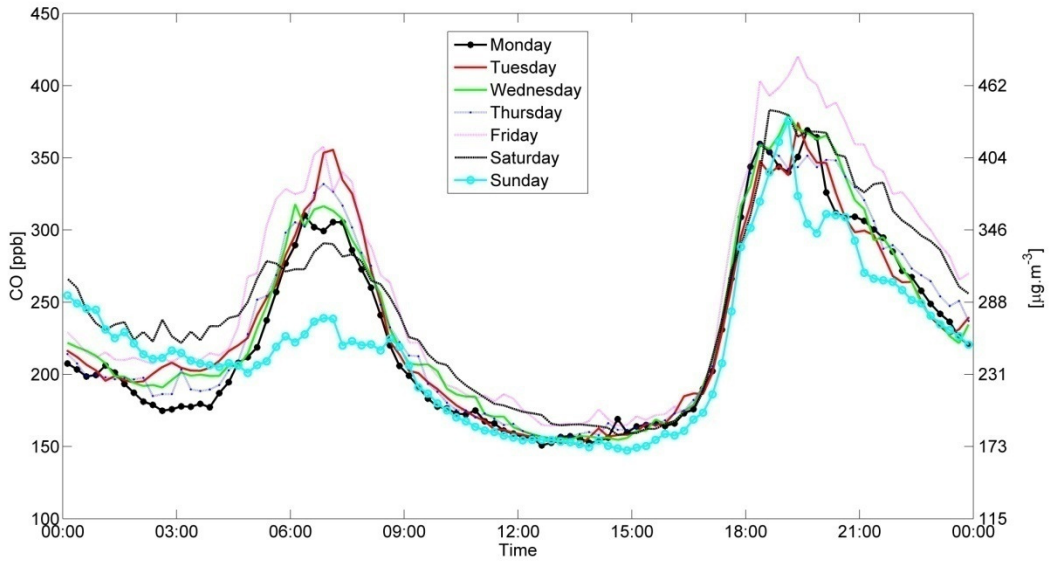

Figure 4.16: Mean daily diurnal CO concentrations

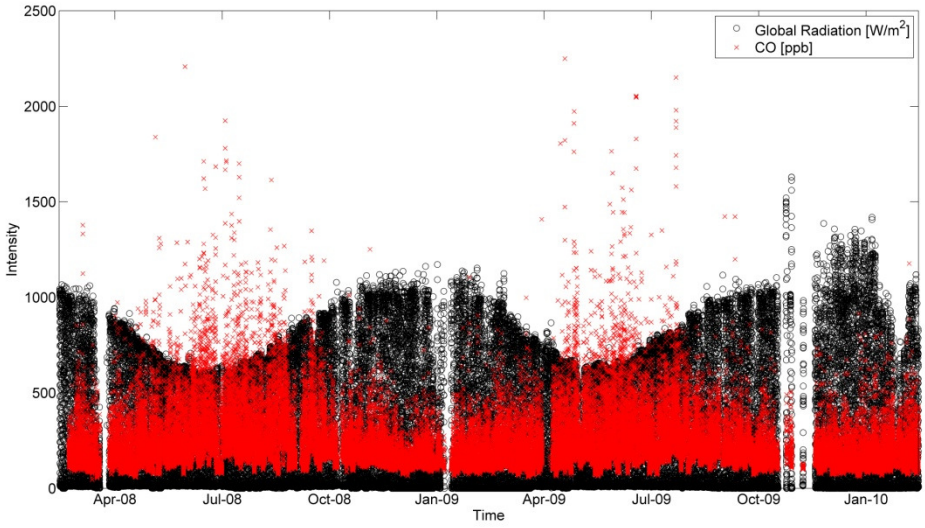

Figure 4.17: Global radiation and CO concentrations are inversely related

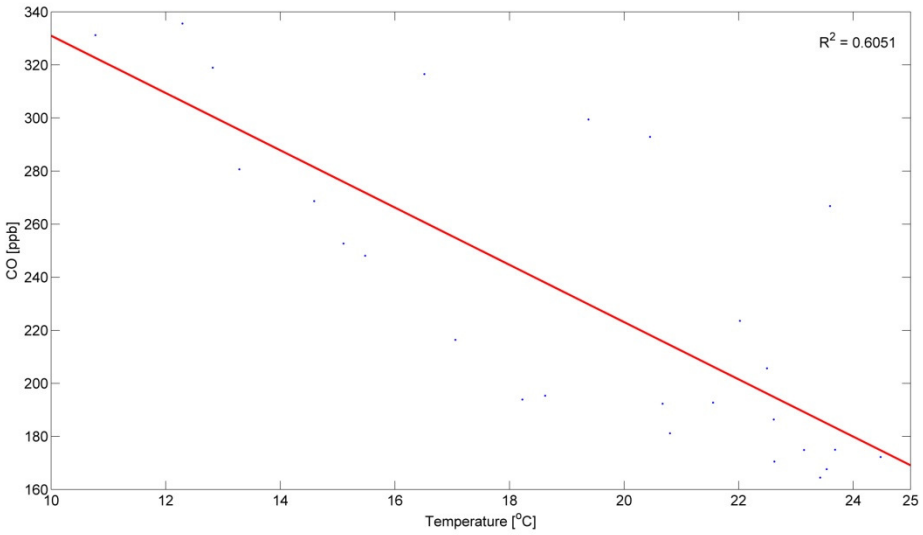

Figure 4.18: Correlation between average monthly CO and average monthly temperatures during the sampling period

Additionally, it is indicated in Figure 4.17 that as the incoming radiation subsides, i.e. in winter, temperatures begin to drop and more CO is generated (Figure 4.18) by cooking and space heating in the informal settlements.

4.6. PM_{10}

The current South African and European 24-hour average standards for PM_{10} are 120µm/m^3 and 50µm/m^3, respectively. For the sampling period in this measurement campaign, South African legislation allowed nine tolerable exceedances (4 p.a.), while European legislation allowed 80 tolerable exceedances (35 p.a.). In 2015, the South African standard will change to 75µm/m^3 and would have allowed nine tolerable exceedances for this sampling period (4 p.a.). In Table 5, the PM_{10} measured is compared to standard concentrations. The mean 24-hours average PM_{10} concentration for the entire sampling period was 44µm/m^3 and the highest 24-hour average PM_{10} concentration measured was 222µm/m^3. During the sampling period, the current and future South African standards were exceeded 15 (6.6 p.a.) and 96 (42.3 p.a.) times, respectively,

while the European standard was exceeded 273 (120.2 p.a.) times. The maximum annual average concentration for the sampling period was 46µgm/m^3, which is above the 2015 South African and current European 40µm/m^3 standard. The number of 24-hour average PM_{10} concentration exceedances, together with the mean annual average PM_{10} levels, clearly indicates the magnitude of PM_{10} pollution in this area.

Table 4.6: Comparison of measured PM_{10} data to South African and European air quality standards listed in Table 4.1

	Measurements					
Averaging period	**Average exceedances per year**		**Sampling period max [ppb] (µg/m^3)**	**Sampling period min [ppb] (µg/m^3)**	**Sampling period average [ppb] (µg/m^3)**	**% data coverage**
	SA	**EUR**				
24 hours	6.6	120.18	(222)	(4)	(44)	87
24 hours (2015)	42.26		(222)	(4)		
1 year	0	n/a	(46)	(44)		
1 year (2015)	0.88		(46)	(44)		

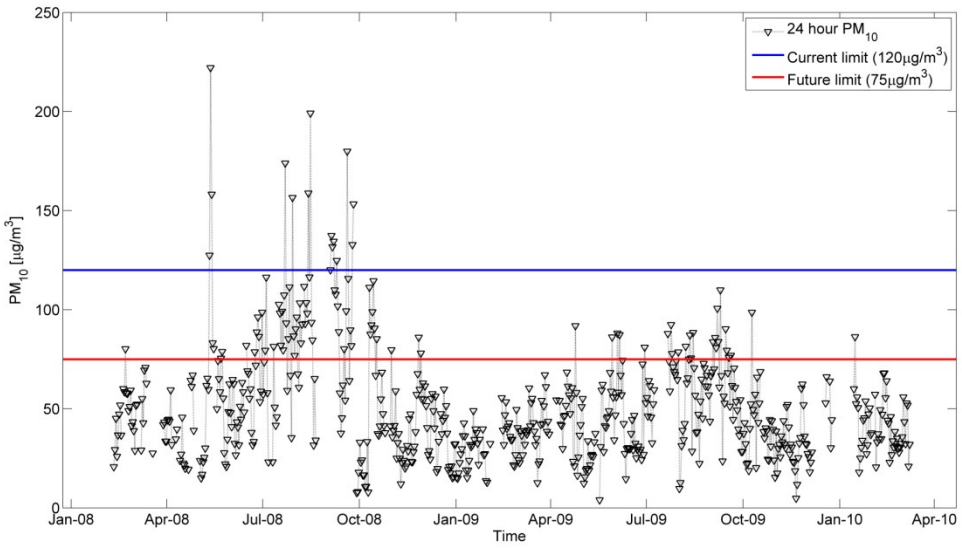

Figure 4.19: The 24 hour mean PM_{10} concentrations for the sampling period shown exceeding the current (blue) and future (red) limits set by government

As indicated, the PM_{10} diurnal seasonal cycle had a peak between 06:00 and 10:00, as well as a second peak between 17:00 and 22:00 (Figure 4.20). The most likely source for atmospheric PM_{10} is identified as household combustion, due to similar bimodal peak periods observed for CO and BC (Figure 4.21). As was expected, the PM_{10} concentrations were also higher during the winter months.

In Figure 4.22, the PM_{10} diurnal trend for each day of the week is presented. This is similar to the patterns observed for CO, NO_2 and BC, which were also attributed to household combustion for cooking and space heating as the major source.

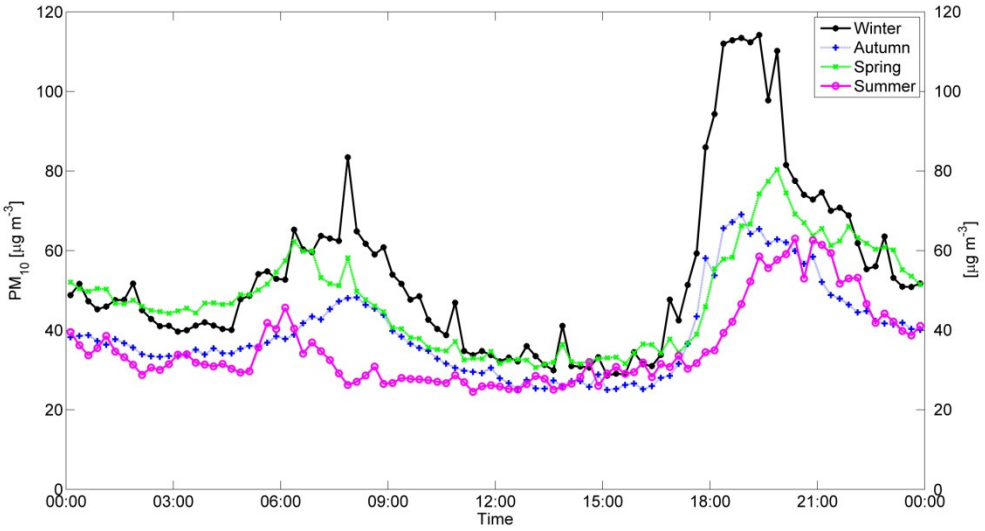

Figure 4.20: Mean diurnal seasonal patterns for PM_{10} (Winter: June, July, August; Spring: September, October, November; Summer: December, January, February; Autumn: March, April, May)

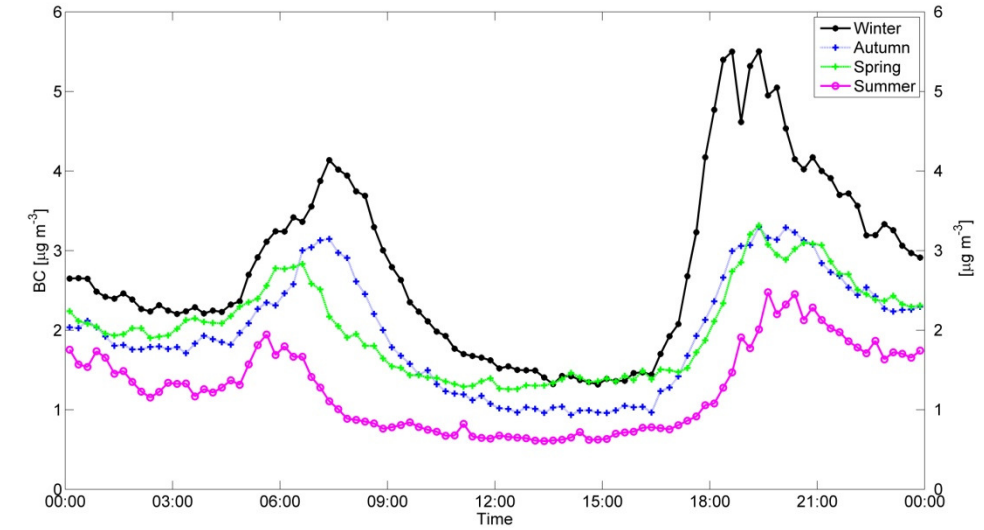

Figure 4.21: Mean diurnal seasonal patterns for BC (Winter: June, July, August; Spring: September, October, November; Summer: December, January, February; Autumn: March, April, May)

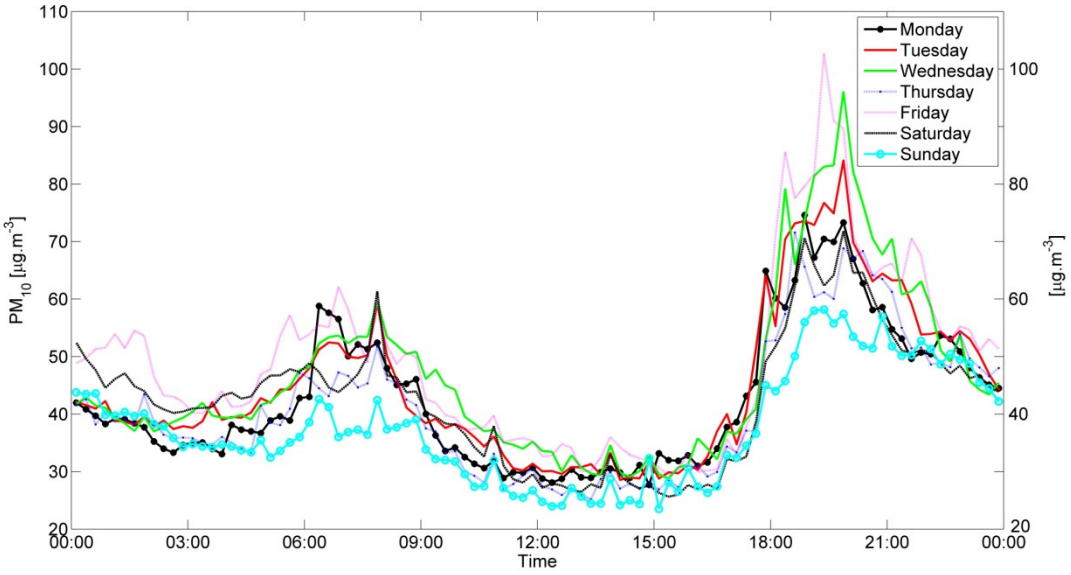

Figure 4.22: Mean daily diurnal PM_{10} concentrations

In the discussion of CO the most likely pollution source was expected to be local household combustion. This explanation is also confirmed by similar diurnal seasonal patterns observed for PM_{10} and BC in Figures 4.20 and 4.21 as these species are also associated with household combustion. PM_{10} and BC also exhibited bimodal diurnal peaks, with the second peak being more pronounced in winter. Additionally, there was an inverse correlation between monthly average CO concentrations and monthly average temperatures (Figure 4.18). Therefore, lower temperatures result in more household combustion, thereby leading to higher CO levels.

4.7. Conclusions

By comparison of the results obtained during this investigation with South African and European air quality standards, it is evident that SO_2, NO_2 and CO concentrations in the western BIC, or at least at this specific measurement site, are in general acceptable. Considering the amount of potential large point sources of these species in this area, the afore-mentioned results were somewhat unexpected, but good (considering human health and environmental impacts). Although no significant exceedances were recorded for SO_2,

NO_2 and CO, the major contributing sources could be identified as high-stack industry emissions for SO_2, and household combustion for NO_2 and CO.

In contrast, O_3 and PM_{10} frequently exceeded standards. O_3 exceeded the eight-hour moving average standard of 61ppb 732 times during the 27 months and nine-days sampling period with an average of 322 times per year. The main contributing factor was identified to be regional sources, with high O_3 precursor species concentration. This problem can only be solved by reducing the regional sources of O_3 precursors (e.g. NO_2 and CO). Currently, vast areas of southern Africa are annually burned during the dry season, while low-income households rely heavily on coal and wood combustion for cooking and space heating. The vehicular fleet in South Africa is relatively old and public transport is not readily available. Additionally, almost no large industries currently de-NO_x, notwithstanding that South Africa is well known for its NO_2 hotspot over the Highveld Airshed Priority Area.

PM_{10} exceeded the current South African 24-hour standard of 120µg/m^3 6.6 times per year, while the future 2015 standard of 75µg/m^3 was exceeded 42.3 times per year. The European 24-hour standard of 50µg/m^3 was exceeded 120.2 times per year. The overall PM_{10} average concentration for the entire sampling period of 44µg/m^3 exceeded the current European and future (2015) South African annual average standard of 40µg/m^3, emphasising the particulate matter pollution problem in the western BIC. The main source of PM_{10} was identified as local household combustion. This can only be rectified by socio-economic upliftment of low-income groups.